Bull. Nov. Comp. Center, Num. Anal., 13 (2005), 47–55

On monotone reconstruction of difference solution at isolated discontinuity*

O.A. Kovyrkina, D. Kroener, V.V. Ostapenko

Abstract. We propose a special monotone reconstruction algorithm in which the monotone property of a high order scheme is improved with the help of the monotone first order scheme. The algorithm provides spreading the shock only at one grid point and ensures second order of the integral convergence through the shock in L_1-norm.

1. Introduction

Currently, the shock-capturing high order accuracy difference schemes as applied to hyperbolic systems of conservation laws are wide-spread [1, 2]. However, in most studies focused on the development of such schemes, the accuracy of a scheme is interpreted as degree of the corresponding Taylor series for smooth solutions. It was shown in [3] that this interpretation does not ensure that a similar increase in the order of weak approximation is attained for discontinuous solutions. Nevertheless, it has long been erroneously believed that schemes retain high order of convergence for every smooth part of an approximated weak solution. In [4–6], it was shown that most of practically used high order difference schemes are really at best of first order of convergence in the domain of an unsteady shock influence. It appeared that quite a resistant opinion is being to be formed that construction of the shock-capturing high order difference schemes, reserving a high order of convergence in the domain of an unsteady shock influence is principally impossible (for the first time this point of view was expressed in [7]).

In [8], it was shown that an improvement in translation of the Hugoniot relations across an unsteady shock requires a difference scheme ensuring a high order of weak approximation with respect to its finite difference solutions. Also, in [8] it was shown that explicit two-layer temporal difference schemes (such as TVD, ENO, NED) can have only the first order of weak approximation. As a result, the schemes approximate the Hugoniot relations accurate to the first order at best, and so they will decrease their order of convergence to the first one in all the region of shock influence independent of their formal order of approximation in the smooth solution. In this paper, an implicit three-layer temporal difference scheme was constructed with a

*Supported by Russian Education Federal Department, Grant A04–2.8–212.

high order artificial viscosity which has the third order of approximation both in the classical and in a weak sense. This new scheme conserves a high order of convergence in all the smooth part of the calculated weak solutions.

Unfortunately, the main deficiency of the proposed scheme is its non-monotonicity and it is impossible to improve this attribute of the new scheme by the standard way (dealing with different flux correcting procedures) without loss of its high order of weak approximation. Therefore in this paper we propose a special monotone reconstruction algorithm in which the monotone property of a high order scheme is improved with the help of the monotone first order scheme. The algorithm is exposed on a simple example of two finite difference schemes for the linear transport equation. One of these schemes is a non-monotone second order Lax–Wendroff scheme and the other is the monotone first order scheme with artificial viscosity. The proposed monotone reconstruction algorithm provides spreading of the shock only at one grid point and ensures the second order of the integral convergence through the shock in L_1-norm.

2. Description of monotone reconstruction algorithm

Let us consider the linear transport equation

$$w_t + w_x = 0 \tag{1}$$

with the initial data

$$w(x,0) = F(x), \tag{2}$$

where $F(x)$ is a piecewise-smooth function that has one discontinuity of the first kind. The exact solution to problem (1), (2) is $w(x,t) = F(x-t)$.

Approximate equation (1) by the Lax–Wendroff scheme of second order

$$\frac{u_j^{n+1} - u_j^n}{\tau} + \frac{u_{j+1}^n - u_{j-1}^n}{2h} = \frac{\tau}{2}\frac{u_{j+1}^n - 2u_j^n + u_{j-1}^n}{h^2} \tag{3}$$

and the first order scheme with a linear artificial viscosity

$$\frac{v_j^{n+1} - v_j^n}{\tau} + \frac{v_{j+1}^n - v_{j-1}^n}{2h} = C\frac{v_{j+1}^n - 2v_j^n + v_{j-1}^n}{h}, \tag{4}$$

where $u_j^n \sim u(jh, n\tau)$, $v_j^n \sim v(jh, n\tau)$ are grid functions, h and τ are the space and the time steps, $C > 0$ is the artificial viscosity coefficient. If function (2) has a discontinuity at the point $\overline{x}_0 = j_0 h$, we approximate the initial data by the following formula:

$$u_j^0 = v_j^0 = \begin{cases} F(jh), & j \neq j_0, \\ \dfrac{F(j_0 h - 0) + F(j_0 h + 0)}{2}, & j = j_0. \end{cases} \tag{5}$$

From the monotonicity criterion [9] we obtain that scheme (3) is non-monotonous and scheme (4) is monotonous under the condition

$$\frac{1}{2} \le C \le \frac{1}{2\lambda}, \quad \lambda = \frac{\tau}{h} < 1.$$

In this paper $h = 0.1$, $\tau = 0.035$, $\lambda = 0.35$, and $C = 0.75$ that ensures the Courant stability condition for schemes (3), (4) and monotonicity of scheme (4).

Let us describe the monotone reconstruction algorithm for one time step from $t = 0$ to $t = \tau$. Assume that we calculate the numerical solutions u_j^1 and v_j^1 of difference problems (3), (5) and (4), (5). So, scheme (3) is non-monotone and scheme (4) is monotone, therefore the following inequalities are valid

$$|u_j^1 - v_j^1| < \varepsilon \quad \forall j \notin [k,l], \quad |u_j^1 - v_j^1| > \varepsilon \quad \forall j \in [k,l], \tag{6}$$

where the discontinuity point $\overline{x}(\tau) = \overline{x}_0 + \tau$ belongs to the interval (kh, lh) and $\varepsilon = O(h)$ is small (here $\varepsilon = 0.01$). In formula (6), $[k,l]$ is integer interval.

Let us construct a new function

$$\omega_j^{1,0} = \begin{cases} u_j^1, & j \notin [k,l], \\ v_j^1, & j \in [k,l] \end{cases} \tag{7}$$

and improve its sharpening with a shock by the following way. We consider the linear extrapolation at the grid points u_{k-2}^1 and u_{k-1}^1 to the right

$$u_k(x) = u_{k-1}^1 + \frac{u_{k-1}^1 - u_{k-2}^1}{h}(x - x_{k-1}), \quad x > x_{k-1}, \tag{8}$$

and at the grid points u_{l+1}^1 and u_{l+2}^1 to the left

$$u_l(x) = u_{l+1}^1 + \frac{u_{l+2}^1 - u_{l+1}^1}{h}(x - x_{l+1}), \quad x < x_{l+1}, \tag{9}$$

where $x_j = jh$. Let us calculate the differences

$$\delta_k = \omega_k^{1,0} - u_k(kh), \quad \delta_l = \omega_l^{1,0} - u_l(lh) \tag{10}$$

and find a minimum of their modules

$$\delta = \min(|\delta_k|, |\delta_l|). \tag{11}$$

Then we change the values $\omega_k^{1,0}$ and $\omega_l^{1,0}$ by the formulas

$$\overline{\omega}_k^{1,0} = \omega_k^{1,0} - \delta \operatorname{sign} \delta_k, \quad \overline{\omega}_l^{1,0} = \omega_l^{1,0} - \delta \operatorname{sign} \delta_l \tag{12}$$

and reconstruct the function (7):

$$\omega_j^{1,1} = \begin{cases} u_j^1, & j \notin [k,l], \\ \overline{\omega}_j^{1,0}, & j = k,l, \\ v_j^1, & j \in [k+1,l-1]. \end{cases} \tag{13}$$

For the case $\delta = |\delta_l|$, the point $\omega_l^{1,1} = \overline{\omega}_l^{1,0}$ of the reorganized function (13) lies on line (9). So, we exclude this point from the process of reconstructing function (13) and continue this process on the diminishing grid interval $[k, l-1]$. For the case $\delta = |\delta_k|$, the point $\omega_k^{1,1} = \overline{\omega}_k^{1,0}$ of the reorganized function (13) lies on line (8). So, we exclude this point from the process of the reconstruction of function (13) and continue this process on the diminishing grid interval $[k+1, l]$. Repeating the reconstruction algorithm (10)–(13) $s = l - k$ times, we obtain the optimal (in the sharpening sense) function $\omega_j^{1,s}$, for which only a certain point $\omega_m^{1,s}$ $(m \in [k,l])$ among all the points $\omega_j^{1,s}$ $(j \in [k,l])$ does not belong to one of the two lines: (8) and (9). We introduce the notation $\omega_j^1 = \omega_j^{1,s}$ for the resulting function of the monotone reconstruction algorithm at the first time step.

Let us continue the algorithm to the second time step from $t = \tau$ to $t = 2\tau$. For this we set $u_j^1 = v_j^1 = \omega_j^1$ and calculate the values u_j^2 and v_j^2 by schemes (3) and (4), respectively. Then we construct the function $\omega_j^{2,0}$ using the numerical solutions u_j^2 and v_j^2. This function is similar to function (7). After that, we repeat the monotone reconstruction algorithm and obtain the resulting function ω_j^2 at the second time step. Repeating this procedure n times, we obtain the reconstructed numerical solution ω_j^n at the n-th time step.

3. The first example

Let us consider the following initial data (2)

$$w(x,0) = \Theta(\overline{x}_0 - x) = \begin{cases} 1, & x < \overline{x}_0, \\ 0, & x \geq \overline{x}_0, \end{cases} \tag{14}$$

where $\Theta(x)$ is the Heaviside function. The exact solution to problem (1), (14) is a shock

$$w(x,t) = \Theta(t + \overline{x}_0 - x) = \begin{cases} 1, & x < \overline{x}_0 + t, \\ 0, & x \geq \overline{x}_0 + t, \end{cases}$$

moving with the speed $D = 1$ to the positive direction of x–axis.

Let us assume that $\overline{x}_0 = 1$. Figures 1 and 2 show the results obtained at the moment $T = 5.005$ by the Lax–Wendroff scheme and by the scheme with

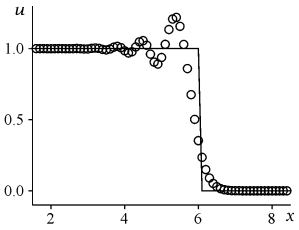

Figure 1

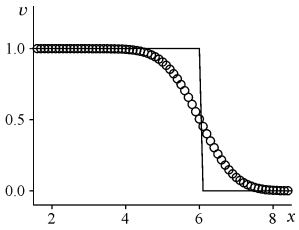

Figure 2

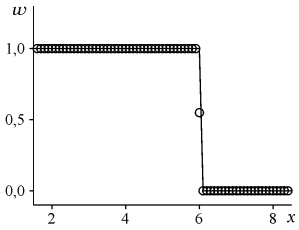

Figure 3

a linear artificial viscosity, respectively. Here and below in all the figures with label (a) the solid curves correspond to the exact solution and the circles represent the corresponding numerical solution. The Lax–Wendroff scheme (3) is non-monotone, therefore the numerical solution u_j^n has oscillations at the shock front. The numerical solution obtained by the scheme with the linear artificial viscosity (4) is monotone, but smears out the shock.

The results of calculations with the use of the monotone reconstruction algorithm are illustrated by Figure 3. We can prove that if the parameter ε in formulas (6) is taken so as to satisfy the inequality

$$\varepsilon < \delta_1 = \lambda(1-\lambda)/2, \tag{15}$$

then the reconstruction algorithm is correct in this case. In this paper, $\varepsilon = 0.01$, $\lambda = 0.35$, and $\delta_1 = 0.2275$, therefore inequality (15) is valid. We can see from Figure 3 that the solution ω_j^n obtained by the monotone reconstruction algorithm has no oscillations and spreads the shock only at one grid point. This spreading is optimal, because when we know the vertical position of the point that lies on the shock, we can restore the exact position of the shock.

4. The second example

Let us consider the initial data

$$w(x,0) = \begin{cases} \sin x + 2, & x \le \overline{x}_0, \\ \sin(x+\Delta x) + 2, & x > \overline{x}_0. \end{cases} \tag{16}$$

The exact solution of problem (1), (16) is the following function:

$$w(x,t) = \begin{cases} \sin(x-t) + 2, & x \le \overline{x}_0 + t, \\ \sin(x-t+\Delta x) + 2, & x > \overline{x}_0 + t. \end{cases} \tag{17}$$

We carry out the calculations for $\overline{x}_0 = 1.7$, $\Delta x = 2.3$ and for $\overline{x}_0 = 4.9$, $\Delta x = 2.1$. The initial difference functions (5) for these cases are shown in Figures 4 and 5. Figures 6–8 and 9–11 represent the numerical results at

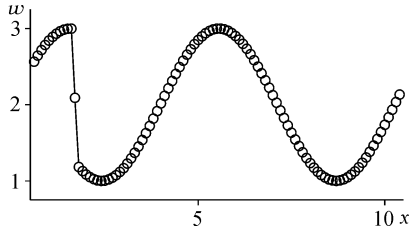

Figure 4

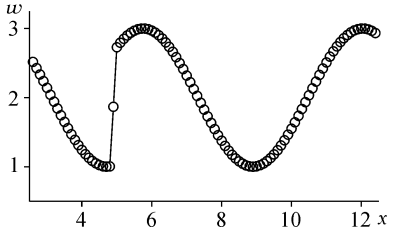

Figure 5

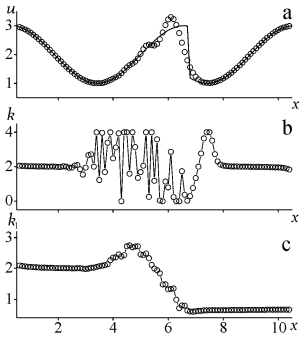

Figure 6

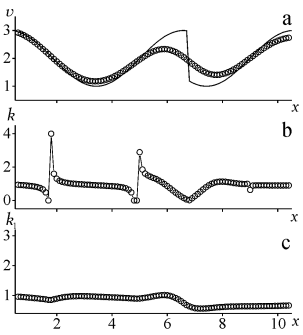

Figure 7

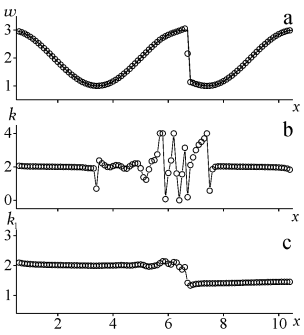

Figure 8

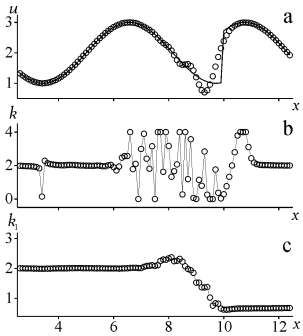

Figure 9

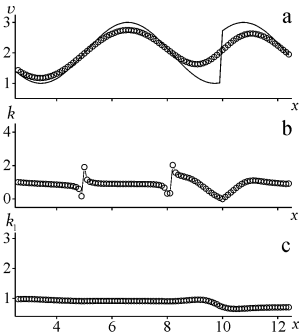

Figure 10

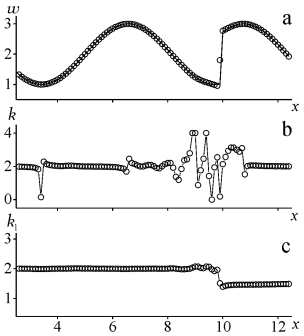

Figure 11

the moment $T = 5.005$ for the initial data, illustrated by Figures 4 and 5, respectively. Figures 6, 9 show the results, obtained by the Lax–Wendroff scheme, Figures 7, 10 — by the scheme with a linear artificial viscosity, and Figures 8, 11 — by the monotone reconstruction algorithm.

The figures with label (a) show the numerical solution as it is. The figures with label (b) represent the local order of convergence with respect to x for all our schemes. To determine the order, we carry out additional calculations with the step $h_2 = h/2 = 0.05$ and $\tau = \lambda h_2 = 0.0175$. The local order of convergence at the point $x_i = ih$ at the moment $t = t_n = n\tau$ is given by the formula (Runge's rule)

$$k(x_i,t)=\log_2\left|\frac{w_{h_1}(x_i,t)-w(x_i,t)}{w_{h_2}(x_i,t)-w(x_i,t)}\right|,$$

where $w(x,t)$ is the exact solution (17), $w_{h_1}(x,t)$ is the numerical solution, obtained by the scheme with the step $h_1=h$ and $w_{h_2}(x,t)$ is the solution, obtained by the scheme with the step h_2.

The figures with label (c) show the order of convergence with respect to $L_1[0,x_i]$ norms, where $0\le i\le N$, $(N+1)$ is the number of grid points on x-axis. The order on the interval $[0,x_i]$ at the moment $t=t_n$ is given by the formula

$$k_1(x_i,t)=\log_2\frac{\|w_{h_1}(x,t)-w(x,t)\|_i}{\|w_{h_2}(x,t)-w(x,t)\|_i},$$

where $\|g(x,t)\|_i=\int\limits_0^{x_i}|g(y,t)|\,dy$ is the norm in $L_1[0,x_i]$, calculated by the trapezoidal rule. At the right boundary $x_N=Nh$ we have the order of convergence in L_1-norm on the whole interval $[0,x_N]$.

5. Another method of calculation of order in L_1-norm

It is clear from Figures 6–8 and 9–11 that the new combined scheme has order (local and in L_1-norm) higher than the Lax–Wendroff scheme. Let us note that this order in L_1-norm decreases through the shock (see Figures 8c, 11c). Probably, this is not due to the algorithm itself, but due to the calculation of the order of convergence. The monotone reconstruction algorithm, described in Section 2, is completed if there remains only one point on the shock front. This point is necessary to keep information about the shock position for the next step of the algorithm. But before defining the order, we can move this point according to the localization algorithm. The results obtained in this case are represented by Figures 12 and 13. We can see the improvement of order in L_1-norm from the comparison of Figures 8 and 11 with Figures 12 and 13.

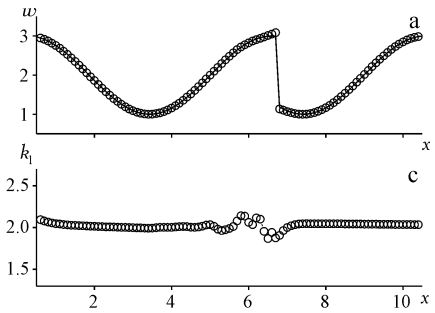

Figure 12

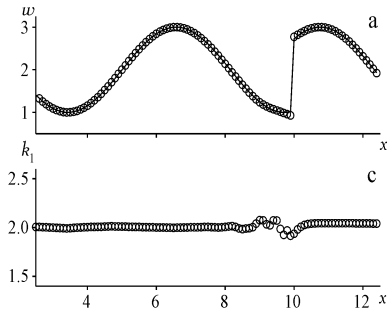

Figure 13

6. The order of convergence, depending on time

Let us analyze the behavior of the order of convergence in L_1 norm for the monotone reconstruction algorithm. We have observed that order strongly varies if we slightly change the time of calculation. For example, if we carry out calculations at the moment $T = 4.97$ instead of the moment $T = 5.005$ (i.e. we subtract one time step τ), then we obtain Figure 14 instead of Figure 8c.

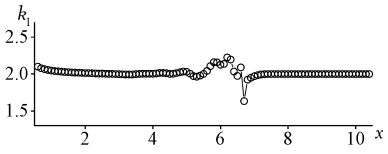

Figure 14

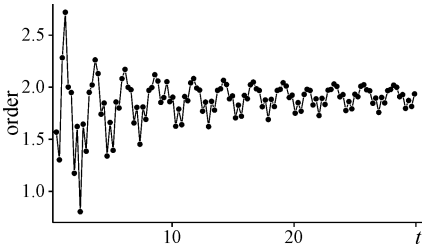

Figure 15

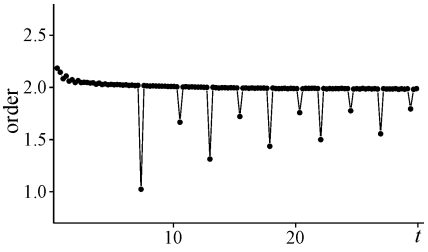

Figure 16

We have decide to analyze the order of convergence in L_1-norm as function of time, for the initial data, illustrated by Figure 4. Figures 15, and 16, show the order of convergence in $L_1[0, x_N]$ norm at successive time moments $\bar{t}_i \in [0, T]$, $T = 857\tau = 29.995$ with the step $\Delta t = \bar{t}_{i+1} - \bar{t}_i = 7\tau = 0.245$. Figure 15 represents a standard method of calculating order, and Figure 16 illustrates the modified method, described in the previous section. We can see from Figures 15 and 16 that both methods give approximately second order of convergence. But the convergence of the modified method is somewhat better. The average orders of these methods with respect to time are calculated by the following formula:

$$K = \frac{1}{M} \sum_{i=1}^{M} k_1(x_N, t_i), \quad M = T/\tau = 857.$$

In the case of the ordinary method $K = 1.85$, and in the case of the modified method $K = 1.98$. So, the monotone reconstruction algorithm allows us to obtain approximately the second order of integral convergence in L_1 norm through the shock.

7. Conclusion

The proposed monotone reconstruction algorithm has shown a high resolution on a simple example of the numerical calculation for the linear transport equation. Let us hope that after a proper adaptation the algorithm can be

used for the monotone reconstruction of the new compact scheme offered in [8] with the help of one of high resolution monotone schemes.

References

[1] LeVeque R.J. Numerical Methods for Conservation Laws. — Basel etc.: Birkhauser, 1992.

[2] Kroener D. Numerical Schemes for Conservation Laws. — Stuttgart: Wiley; Teubner, 1997.

[3] Ostapenko V.V. Approximation of conservation laws by means of shock-capturing finite-difference schemes // Comput. Maths. Math. Phys. — 1990. — Vol. 30, No. 9. — P. 91–100.

[4] Ostapenko V.V. Convergence of finite-difference schemes behind a shock front // Comput. Maths. Math. Phys. — 1997. — Vol. 37, No. 10. — P. 1161–1172.

[5] Casper J., Carpenter M.N. Computational consideration for the simulation of shock-induced sound // SIAM J. Sci. Comput. — 1998. — Vol. 19, No. 3. — P. 813–828.

[6] Engquist B., Sjoegreen B. The convergence rate of finite difference schemes in the presence of shocks // SIAM J. Numer. Analysis. — 1998. — Vol. 35, No. 6. — P. 2464–2485.

[7] Ivanov M.Ya., Kraiko A.N. Approximation of discontinuous solutions in shock-capturing computations // Comput. Maths. Math. Phys. — 1978. — Vol. 18, No. 3. — P. 780–783.

[8] Ostapenko V.V. Construction of high-order accurate shock-capturing finite-difference schemes for unsteady shock waves // Comput. Maths. Math. Phys. — 2000. — Vol. 40, No. 12. — P. 1784–1800.

[9] Godunov S.K. A finite-difference method for numerical analysis of discontinuous solutions in fluid dynamics // Mat. Sb. — 1959. — Vol. 47, No. 3. — P. 271–306.